



Methods of Determining Bubble and Dew Points of Oil and Gas Confined in Nanopores

Kaitlyn Elizabeth Ray Stapp

Department of Petroleum Engineering, *University of Wyoming*

Advisor: Morteza Dejam, Ph.D.

Fall 2020

Abstract

Unconventional shale reservoirs hold promising futures as energy resources, though their oil and gas recovery can be significantly altered by the presence of nanopores. There is a limited number of studies conducted on the effects of nanoconfinement on bubble and dew points of reservoir fluids. These experiments were typically performed on pure compounds or based on theory and empirical approaches. Therefore, experimental studies of efficiently and accurately identifying the phase behavior of confined fluids are strongly needed in the industry. Recently there have been new isochoric methods developed using Differential Scanning Calorimetry (DSC) to measure the behavior onset of vapor-liquid phase transitions. This has been applied to the measurement of the vapor pressure of CO₂ and dew points of a binary gas mixture. In addition, there has been success in an isochoric two-phase bubble point pressure method in finding the vapor pressures of methanol. This research has found that isochoric methods are superior to the more common isobaric methods, and can be more widely applied to various compounds and mixtures. These new methods have great applications for phase behavior of confined fluids in unconventional formations. This research in general will explore and discuss the isochoric methods and their benefits.

Methods of Determining Bubble and Dew Points of Oil and Gas Confined in Nanopores	3
---	---

Contents

Abstract	2
Introduction	4
Problem Definition	6
Solution Methodology	7
Results and Discussion	9
Summary and Conclusion	13
Acknowledgements	14
References	15

Introduction

Energy in today's day and age is more complicated and intricate in nature than ever. Renewable energy or fossil fuels? Wind turbines or solar power? Oil and gas has been a reliable and large-scale energy resource for years and has formulated society as we know it. As we continue to look for innovative ways to revolutionize the oil and gas industry, we further delve into the realm of unconventional shale hydrocarbon production. Locations such as the Western Canadian Sedimentary Basin¹ and the Horn River Basin² hold promising futures in increased gas production as access to conventional sources inevitably dwindle over time. Shale reservoirs are utilized as a primary source of hydrocarbons in today's oil and gas industry, after production of natural gas from shale dramatically increased in the early 2000's. Production of hydrocarbons from shale reservoirs has been steadily increasing since its introduction, with dry shale gas production in the United States reaching 70.62 Bcf/d as of September 2020, as compared to 19.2 Bcf/d ten years prior³.

When observing these particular formations as noted above, shale reservoirs as opposed to conventional gas formations are formulated by tight formations of nanopores⁴. Though industry interest is piqued, there is a lack of sufficient experimental data that can provide an adequate understanding of the behaviors of fluids existing under these enigmatic conditions. In particular, the phase behavior of oil and gas confined in nanopores is still largely considered only through experimental procedures, simulations, and theory⁵. Nanoconfinement can dramatically affect the properties and behaviors of the trapped fluids. It is known that during production of hydrocarbons, decreasing pressure and altered phase behavior can be observed and demonstrated across a P/T graph and phase envelope diagram. Fluid composition, in addition to reservoir pressure, can help in determining the phase behavior - in turn this affects the bubble and dew points of the fluids in question. The performance of a reservoir is highly dependent on the observed phase behavior, as, for example, oil recovery is maximized with a pressure maintained above the bubble point curve⁶.

With the limited amount of studies that have been conducted, the measurement of these phase transitions has not been explored in depth. Not only are studies of this nature beneficial to unconventional shale formation hydrocarbon production, but it also has applications in other industries, including the CO₂ capture by using nitrogen-enriched nanoporous polytriazines (NENPs)⁷. The development and execution of experimental studies of phase behavior of confined fluids are still urgently needed, in particular for reservoir engineering applications, as current studies are not sufficient to maximize an understanding of the fluid behavior in unconventional nanoporous formations. The various experiments that have been conducted in assorted fields are mostly concerned with the utilization of pure compounds. There have been multiple studies completed to a great extent utilizing mesoporous silica-based materials such as SBA-15, KIT-6, and MCM-41^{8, 9, 10, 11, 12} and experimental methods involving the consideration of nanoconfinement in single molecule imaging¹³, hydrogen storage¹⁴, catalysis, ion-exchange¹⁵,

x-ray diffractions, and differential scanning calorimetry (DSC)¹⁶. In addition, studies have been conducted for the phase behaviors of water and small molecule organic liquids in nanoporous medium, which found that the melting and freezing points of these liquids had been decreased¹⁷. This research will aid in identifying various methods of the determination of bubble and dew points of oil and gas confined in nanopores, in particular, studies conducted by Qui et al. involving new isochoric DSC procedures.

Problem Definition

The collection of a reservoir's cumulative gas production and gas reserves, considered as its endowment, varies as it ranges from conventional formations to tight shale formations. As the pore throat apertures and permeability decreases, factors such as the cost of production, time, and necessary research will increase as well. This is a major factor in equating the feasibility of the operation. The said value of an operation and reservoir is partly determined by the negative cash flows from sources such as drilling and production. Streamlining such processes that go into an operation can minimize any unnecessary additional costs, and is done so by fostering a thorough understanding of the target formation and reservoir. A key component to this is the properties of the producing fluids - this includes phase behaviors and bubble and dew point values. Bubble and dew points are used to plan production profiles and are therefore exceptionally vital to any operation¹⁸.

Fluids in confined versus unconfined spaces have major differences in the P/T behavior. There is an increase in capillary forces in smaller pore throats, which can greatly affect the vapor-liquid equilibria and fluid flow dynamics, in addition to the phase behavior¹⁹. There were early studies conducted by Brusilovsky (1992) on the effects of capillary pressure on the vapor-liquid equilibrium in a porous medium. The resulting equation of state (EOS) modeling found that the bubble point will decrease from the bulk point, and dew point will increase from the bulk point under these conditions. It was also concluded that in the presence of variable pore sizes, in larger pores the bubble point is reached first, and in smaller pores the dew point is reached first²⁰. The effects of capillary pressure on phase behaviors was further studied by Nojabaei et al. (2013) and had similar findings, wherein the bubble points had decreased in small pore throats. The variances in the P/T properties of the Bakken shale formation considered in this study directly correlated to discrepancies in its gas-oil-ratio (GOR), for instance. Not properly accounting for changes in capillary pressures can lead to inaccurate oil and gas recovery estimates²¹.

In general, the majority of studies done on phase behaviors on a relatable scale are performed with pure compounds, and are not directly applicable to confined hydrocarbon mixtures. There is a fundamental lack of experimental data exploring these issues, and therefore in demand.

Solution Methodology

Experimental approaches to the phase behavior of oil and gas typically use isobaric methods. However, recently the identification of these properties used isochoric processes instead. In an isochoric process, the identifying factor is the “constant volume”²². Various mesoporous and nanoporous silica materials can be used in these experiments, such as MCM-41, SBA-15, and SBA-16. SBA-15 is a mesoporous silica that is characterized using the Brunauer, Emmett and Teller analysis and contains various pore diameters averaging 8 nm²³.

Studies from Qiu et al. (2019) concerns a new isochoric procedure for vapor-liquid phase transitions using differential scanning calorimetry (DSC), which extends to confined fluids. In this experiment, three SBA-15 samples with varying pore diameters, referred to as samples S1, S2, and S3, and are measured by an analytical balance to be of *ca.* 100 mg. The sample is degassed and moisture and volatile contaminants are desorbed. The samples are cooled to 77.35 K and exposed to nitrogen gas (N₂).

Figure 1(a) demonstrates the N₂ adsorption and desorption isotherms from the three SBA-15 samples. These samples can be defined as *Type IV*, which is characterized by its hysteresis loop, a phenomenon of the input-output graphs²⁴. This occurs from condensation in the mesopores and its high range of relative pressure (P/P_0). The hysteresis of type *H1* will contain a typically uniform array and narrow pore size distribution²⁵. The isotherm is given as the gas volume adsorbed versus this relative pressure. It is shown in Figure 1(a) that the volume (cm³ STP/g) is highest for sample S3 and lowest for sample S1 as the relative pressure increases. This is explored further in Figure 1(b).

Figure 1(b) concerns the pore diameter distribution (determined from the Barrett-Joyner-Halenda (BJH) desorption and adsorption models), which is shown to be roughly ranging between 2 - 10 nm and contain micropores (under 2 nm) as anticipated. Pore size discrepancies are not of a substantial concern, as it is known that the progression of pore sizes increases from S1, to S2, to S3. The smaller the pore size, the greater change or potential change in phase transition properties, as previously mentioned.

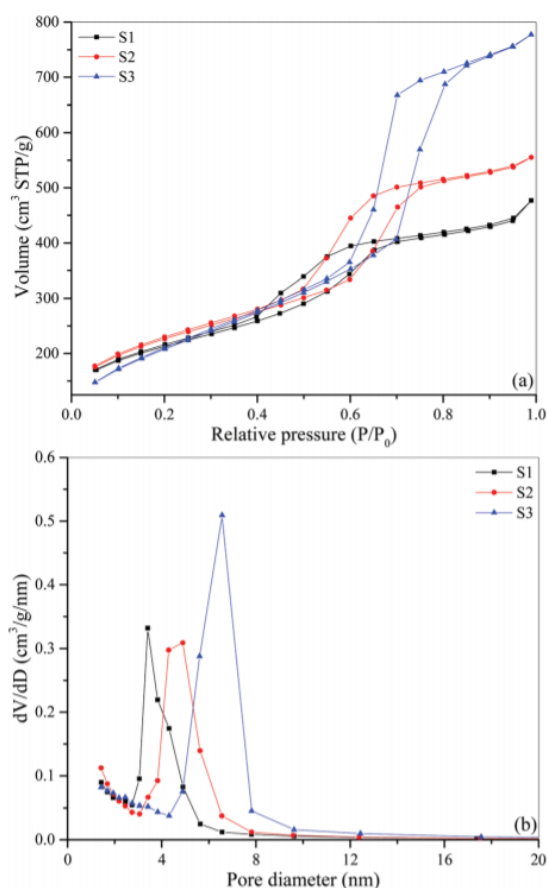


Fig. 1(a): N₂ adsorption-desorption isotherms for SBA-15 samples S1, S2, and S3.

Fig. 1(b): BJH desorption pore size distribution for SBA-15 samples S1, S2, and S3.

In these experiments, when measuring the vapor-pressure of CO_2 and dew points of a $\text{CH}_4/\text{C}_2\text{H}_6$ gas mixture, the initial temperature is maintained above the dew point temperature, and slowly cooled at $0.03\text{ }^\circ\text{C}/\text{min}$ till an exothermic peak is observed on the thermogram and it is returned to ambient conditions. When repeating this procedure for the vapor-pressure of methanol, inert N_2 gas is introduced and the system is heated at a rate of $0.03\text{ }^\circ\text{C}/\text{min}$. After an endothermic peak is observed, it is returned to ambient conditions. This heating process is done so by an isochoric two-phase bubble point measurement. This isochoric process is just as effective as the conventional isobaric methods more typically used. The initial pressure is varied throughout this process and the procedure is repeated for all gases for four vapor pressure measurements. The scanning rate of $0.03\text{ }^\circ\text{C}/\text{min}$ is used for DSC scanning. A slow scanning rate is needed to ensure that the system is maintained in equilibrium.

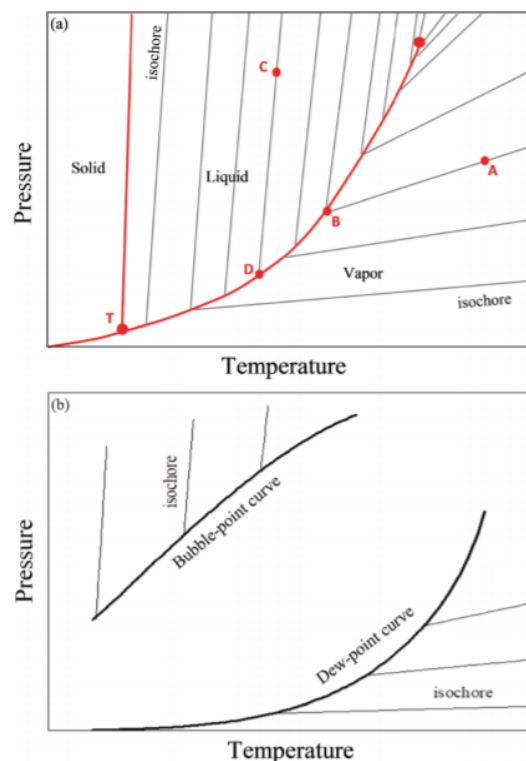


Fig. 2(a): P/T diagrams of a pure component.

Fig. 2(b): P/T diagrams of a mixture with isochores.

In the previous research from Qiu et al. (2018) on this new isochoric procedure for measuring the onset of vapor-liquid transitions, this novel method utilizes cooling in a high-pressure micro-DSC of both pure compounds and gas mixtures, including the binary methane/ethane gas mixture. As opposed to the conventional isobaric methods, the isochoric procedures used are applied to measuring the vapor pressures of methanol on heating to validate its effectiveness. Ideal isochoric DSC measurements can be demonstrated with P/T diagrams and characterized using other behavioral properties.

For a pure component, a typical P/T diagram is shown in Figure 2(a). It is observed that the cooling path will occur along the following isochores. The dew point is denoted by point B through the isochoric dew point measurements, and the bubble point can be found on the path from point C to point D from the isochoric bubble point measurements. This method uses a cooling process to determine these points. In both the isochoric bubble and dew point measurements, the sample must begin in a one-phase region till the phase transition is reached - for the dew point measurements, it begins in a vapor phase till liquid appears, and vice versa for the bubble point measurements.

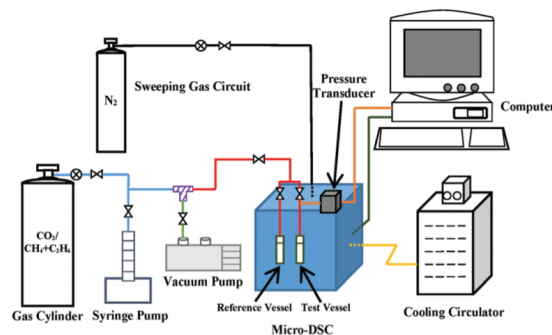


Fig. 3: The experimental apparatus used.

Bubble point measurements are also able to be determined using the isochoric two-phase bubble-point measurement, in which gas and liquid phases coexist. However, this requires truly inert gas which dissolves correctly into a nonvolatile liquid. Figure 2(b) continues this discussion with another P/T diagram for an ideal pure component. At a given composition, Figure 2(b) demonstrates how the bubble and dew point curves envelop the two-phase region as the isochores are followed, until the bubble and dew point curves are reached.

Isochoric processes for measuring the vapor pressure of pure components as well as gaseous mixture dew points are done so experimentally with necessary equipment. Figure 3 shows the details of the apparatus used in this experiment. It contains a high-pressure SETARAM μ DSC VII which operates between the parameters of -45°C and 120°C , under a pressure limit of 400 bar, and a sensitivity resolution of $0.04\ \mu\text{W}$. There are two closed vessels under high pressure for both a controlled reference and to contain the sample. There is a pressure transducer used to measure the pressure on the test sample with a range between 0 to 414 bar ($\pm 0.01\%$). A rotary vane vacuum pump is used to evacuate the sample, while a digital high-pressure syringe pump is used to inject gas to the sample to adjust the pressure. The power rack and thermostatic walls are cooled with a cooling circulator. The pressure and heat flow data collected from the μ DSC is found synchronously.

These studies have aided in the compilation of new information and furthering understanding for nanoconfinement. We will discuss the results and conclusions of these experiments in the following sections.

Results and Discussion

Various methods of experimentation can be applied to the phenomenon of nanoconfinement. Phase behavior of oil and gas can be commonly described with P/T diagrams and phase envelopes. Phase diagrams can be found using equations of state (EOS), such as the popular Peng-Robinson EOS. The Peng-Robinson EOS paired with the capillary pressure equation and adsorption theory has been used in other instances to study the phase equilibria in nanopores of both pure components and mixtures of n-butane, n-pentane, and n-hexane. The smaller the nanopores, the higher the deviation in the vapor-liquid equilibrium. In binary mixtures, it was found that nanoconfinement has increased effects when the difference between components was increased²⁶. Other experiments from Hosein et al. (2014) utilized Constant Mass Expansion (CME) tests and visual observations to determine the bubble and dew points of oil and gas condensates. The CME test was conducted in a windowed PVT cell at initial reservoir pressure and temperature. The dew points were found via observation, pressure-volume relations, and a derived Y-function. However, this is not applicable to oil and gas confined in nanopores and was applied under conventional properties.

Studies conducted by Wang et al. (2014) utilized microfluidic and nanofluidic chips to study multi-phase flows in channels and phase changes. This particular study found that the vaporization of liquid was more suppressed in nanopores when compared to micropores as the liberation of lighter components caused the apparent molecular weight increase in the remaining fluid. After the flash calculation at 345 K, the remaining liquid was composed of 93.25 mol% n-octane (before flash calculation was 80.00 mol%), while it contained 4.53 mol% of the lighter n-butane before flash calculation and 1.87 mol% after²⁷.

Previous experiments from Qui et al. (2018 and 2019) directly concerns the effects of nanoconfinement on dew and bubble points.

Vapor pressure measurements using isochoric procedures for CO₂ and methanol

We can revisit the isochoric procedures from Qui et al. (2019 and 2018) used to determine vapor pressures of CO₂ and methanol at specific temperatures. It is also known that isobaric procedures would be very difficult to use when measuring the vapor pressures of CO₂ due to the volatile nature of CO₂ and difficulty in finding an inert gas that is dissolvable in CO₂. In comparison, these are not of concern for this isochoric process for CO₂.

We can compare the measurements of the vapor pressures and cooling/heating paths for both CO₂ and methanol with NIST data in Figure 4(a) and Figure 4(b). In Figure 4(a) for the vapor pressure of CO₂, as the sample cools and condensates, there is a dramatic increase in the heat flow and a simultaneous decrease in the system pressure. The cooling paths displayed differ from the ideal isochores from variations in temperature outside the test sample. In addition, the average absolute deviation (AAD) from NIST data is under +/- 1%. In Figure 4(b) for the vapor pressure of methanol, it begins with different initial pressures and temperatures for the isochoric

two-phase bubble point measurements. The sample size, pinhole size, and scanning rates are not needed to be optimized. In this experiment, the N_2 gas dissolves sparingly into the mostly liquid, nonvolatile methanol.

Dew points of a methane/ethane gas mixture

This experiment utilized DSC isochoric dew point measurements for methane/ethane gas mixtures, of $15 \pm 0.3\%$ methane and $85 \pm 0.3\%$ ethane. The onset of the phase transition is once again determined by an exothermic peak on the thermogram. From this we can also find the corresponding dew point pressure and dew point temperature.

It is also discussed in other research from Qui et al. (2018) that the DSC scanning rate can affect the dew point measurements. However, though the mixture is in equilibrium, the composition will change as the parameters are altered. The effects of nanoconfinement can significantly alter the gas composition, and would therefore not be reflected accurately. This change in composition is created by the confined fluid adsorption thickness²⁸ and can be minimized by utilization of a variable amount of an adsorbent. However, this should be limited to still allow for noticeable exo/endermic peaks on a thermogram. Changes in the amount of adsorbent in as little as 2.5 mg will change the bulk gas composition greatly. It should be noted that there were amounts of adsorbent of 1.3 mg, 2.2 mg, and 2.0 mg used in this experiment respectfully for S1, S2, and S3. The data found from this isochoric method had an error of ± 0.136 bar or ± 0.167 °C for an exact composition, or ± 0.25 bar when accounting for inconsistencies in gas composition. The data found also aligns well with

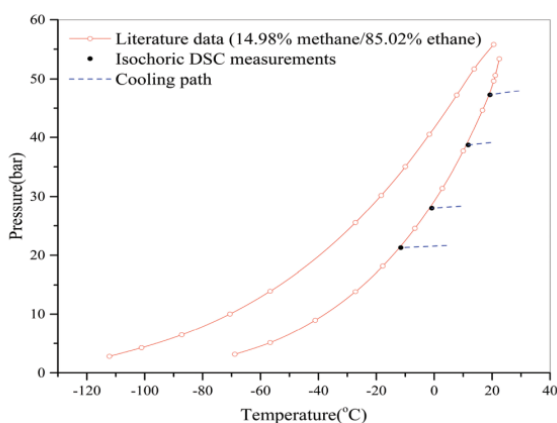


Fig. 5: Measurements of dew points for a methane/ethane mixture.

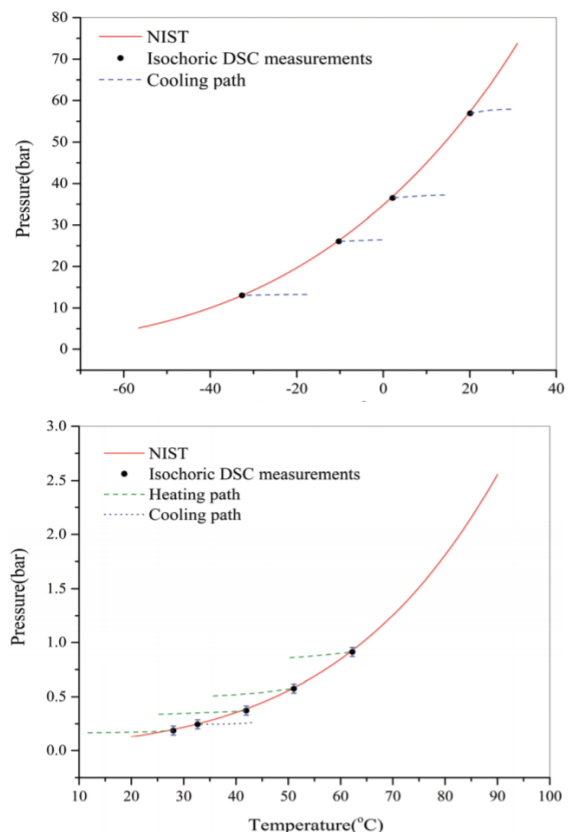


Fig. 4: Vapor pressure measurements and cooling/heating paths of (a) CO_2 and (b) methanol.

literature data. Iconically, this experiment is the first successful usage of DSC to determine dew points of a gas mixture. Though in this experiment it was applied to a binary mixture, it can be used in multicomponent mixtures as well. The P/T diagram shown in Figure 5 also shows the cooling paths and the data found in comparison to the literature data. In this Figure is also shown the dew point measurement results from this experiment²⁹.

Capillary condensation and bulk condensation of CO₂ in SBA-15

If we delve further into the 2018 research from Qui et al., we can further discuss the usage of SBA-15 to find capillary condensation measurements of CO₂. The thermogram from the isochoric dew-point measurements displays two separate exothermic peaks, rather than a single peak as previously discussed. An initial, smaller peak reflects the beginning of the phase transition and a slight drop in the system's pressure. The larger peak reflects the bulk condensation occurring and is also characterized by a much more swift drop in the system's pressure.

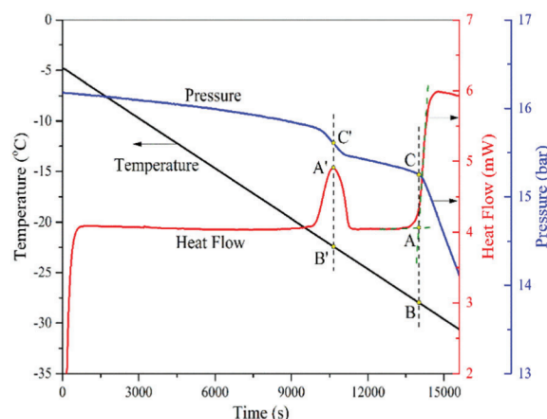


Fig. 6: The thermogram of the capillary condensation and bulk condensation measurements in SBA-15.

As aforementioned, a slow DSC scanning rate is needed, clocked at 0.03 °C/min. However, it should be noted that a scanning rate of 0.1 °C/min is totally sufficient and lowering it further will not guarantee more accurate results. In a single run, the DSC is able to also measure both the capillary condensation and bulk condensation. The bulk phase transition pressure and temperature can be found in the thermograms in Figure 6 from the intersection of the tangential line of the second exothermic peak and the baseline of the heat flow (point A). This pressure (point C) and temperature (point B) is the vapor pressure and condensation temperature of the system. When concerning capillary condensation, we do not determine this in the same manner, as that would only yield results from small mesopores. Instead, we observe the vertical line through the first exothermic peak (point A') and the corresponding intersecting pressure (point C') and temperature (point B')³⁰.

Summary and Conclusion

Methods of determining phase transitions of oil and gas under nanoconfinement are largely lacking. There are various possible methods that can be reapplied correctly to more needed scenarios - this includes CME tests, X-ray scattering, and nanofluidic chips. Mesoporous silica, including KIT-6, MCM-41, and the popular SBA-15, are commonly used as well in such experiments. However, most successful is the recent findings from Qui et al (2018 and 2019) and their utilization of isochoric DSC procedures. This recent research has proven isochoric approaches to be effective in determining vapor-liquid onsets in comparison to conventional isobaric methods. Similar to the isobaric methods, the isochoric two-phase bubble-point measurements contain a liquid in coexistence with an inert gas (N_2). This method measured the vapor pressures of liquid methanol with results in excellent agreement with current literature. This same research continues to utilize the isochoric dew point measurements in SBA-15 to find the capillary condensation of CO_2 , as well as dew points of a methane/ethane gas mixture. This work verifies that as pore sizes decrease, the phase transition boundaries decrease from the bulk fluid boundaries. The DSC has the ability to simultaneously measure the phase transition of both the bulk and confined fluids, which furthers to improve accuracy and fine-tune parameters of the study. In Qui et al.'s 2019 publication, it is the first instance of successfully measuring the vapor-liquid phase transition onset in an isochoric procedure from a high-pressure μ DSC and finding the dew point of a gaseous mixture. This research also continues to find vapor pressures of CO_2 under these conditions.

It can be known that isochoric DSC measurements can be easily and simply applied, and can be more effective than isobaric methods as there is less parameter optimization needed. The thermograms generated are more clear and easily understood. The knowledge found here can be taken and reapplied or distributed to other instances of nanoconfinement in the oil and gas industry, and is a great step closer to redefining unconventional hydrocarbon sources.

Acknowledgements

Kaitlyn Stapp is appreciative of the opportunity from Professor Morteza Dejam, Ph.D., to partake in this research.

References

- 1 Javadpour, F., Fisher, D., Unsworth, M. *Nanoscale gas flow in shale gas sediments*. Journal of Canadian Petroleum Technology, Vol. 46.10, Oct 2007, 5-61.
- 2 Teklu, T. W., Park, D., Jung, H., Miskimins, J. *Integrated Rock Characterization of a Shale Gas Field in the Horn River Basin, Canada*. Unconventional Resources Technology Conference, July 2018.
- 3 U.S. Energy Information Administration (EIA). *Natural gas annual*, September 2020.
- 4 Aguilera, R. *Shale gas reservoirs: Theoretical, practical and research issues*. Petroleum Research, Vol. 1.1, Sept 2016, 10-26.
- 5 Qui, X., Tan, S. P., Dejam, M., Adidharma, H. *Simple and accurate isochoric differential scanning calorimetry measurements: phase transitions for pure fluids and mixtures in nanopores*. Phys. Chem. Chem. Phys., 2019, 21, 224-231.
- 6 Satter, A., Iqbal, G. M. *Phase behavior of hydrocarbon fluids in reservoirs*. Reservoir Engineering: The Fundamentals, Simulation, and Management of Conventional and Unconventional Recoveries, 2016, 107-115.
- 7 Chaudhary, M., Muhammad, R., Ramachandran, C. N., Mohanty, P. *Nitrogen Amelioration-Driven Carbon Dioxide Capture by Nanoporous Polytriazine*. ACS Publications 2019, 35, 14, 4893-4901.
- 8 Wang, D., Sui, J., Qi, D., Deng, S., Wei, Y., Wang, X., Lan, X. *Phase transition of docosane in nanopores*. Journal of Thermal Analysis and Calorimetry, 2019, 135, 2869-2877.
- 9 Vojoudi, H., Badiei, A., Bahar, S., Ziarani, G. M., Faridbod, F., Ganjali, M. R. *Post-modification of nanoporous silica type SBA-15 by bis(3-triethoxysilylpropyl)tetrasulfide as an efficient adsorbent for arsenic removal*. Powder Technology 319 (2017), 271-278.
- 10 Ok, S., Hwang, B., Liu, T., Welch, S., Sheets, J. M., Cole, D. R., Liu, K., Mou, C. *Fluid Behavior in Nanoporous Silica*. Front. Chem., 2020.
- 11 Kleitz, F., Bérubé, F., Guillet-Nicolas, R., Yang, C., Thommes, M. *Probing Adsorption, Pore Condensation, and Hysteresis Behavior of Pure Fluids in Three-Dimensional Cubic Mesoporous KIT-6 Silica*. J. Phys. Chem. C 2010, 114, 20, 9344-9355.
- 12 Szewczyk, A., Prokopowicz, M., Sawicki, W., Majda, D., Walker, G. *Aminopropyl-functionalized mesoporous silica SBA-15 as drug carrier for cefazolin: adsorption profiles, release studies, and mineralization potential*. Microporous and Mesoporous Materials, Vol. 274, 2019, 113-126.
- 13 Dong, B., Pei, Y., Mansour, N., Lu, X., Yang, K., Huang, W., Fang, N. *Deciphering nanoconfinement effects on molecular orientation and reaction intermediate by single molecule imaging*. Nat Commun 10, 4815 (2019).
- 14 Li, B., Huang, X., Liang, L., Tan, B. *Synthesis of uniform microporous polymer nanoparticles and their applications for hydrogen storage*. J. Mater. Chem., 2010, 20, 7444-7450.
- 15 Materazzi, S. *Recent Advances, Techniques, and Applications*. Handbook of Thermal Analysis and Calorimetry, Vol. 5, 2008.
- 16 Huber, P., Soprunyuk, V. P., Knorr, K. *Structural transformations of even-numbered n-alkanes confined in mesopores*. Phys. Rev. E 74, 031610, 2006.
- 17 Yan, X., Wang, T. B., Gao, C. F., Lan, X. Z. *Mesoscopic Phase Behavior of Tridecane–Tetradecane Mixtures Confined in Porous Materials: Effects of Pore Size and Pore Geometry*. J. Phys. Chem. C 2013, 117, 33, 17245–17255.
- 18 Hosein, R., Mayrthoo, R., McCain Jr., W. D. *Determination of Bubble-Point and Dew-Point Pressure without a Visual Cell*. Journal of Petroleum Science and Engineering 124 (2014) 105-113.
- 19 Teklu, T.W., Alharthy, N., Kazemi, H., Yin, X., Graves, R. M., Alsumaiti, A. *Phase Behavior and Minimum Miscibility Pressure in Nanopores*. SPE Reservoir Evaluation & Engineering. Vol 17, 496.
- 20 Brusilovsky, A. I. *Mathematical Simulation of Phase Behavior of Natural Multicomponent Systems at High Pressures with an Equation of State*. SPE Reservoir Eng. 1992,7, 117–122.
- 21 Nojabaei, B., Johns, R. T., Chu, L. *Effect of Capillary Pressure on Phase Behavior in Tight Rocks and Shales*. SPE Reservoir Evaluation & Engineering, Vol 16, 281-289.

- 22 Dalarsson, N., Dalarsson, M., Golubović, L. *Quasi-Static Thermodynamic Processes*. Introductory Statistical Thermodynamics, 2011, Ch. 14, 14.2.
- 23 Grünberg, B., Emmler, T., Gedat, E., Shenderovich, I., Findenegg, G. H., Limbach, H., Buntkowsky, G. *Hydrogen Bonding of Water Confined in Mesoporous Silica MCM-41 and SBA-15 Studied by H Solid-State NMR*. Chemistry - A European Journal, Vol. 10, 22, 2004, 5689-5696.
- 24 Morris, K. *What is Hysteresis?* Applied Mechanics Reviews, 2011, 64, 5, 1001.
- 25 Sing, K. S. W., Everett, D. H., Haul, R. A. W., Moscou, L., Pierotti, R. A., Rouquerol, J., Siemieniowska, T. *Reporting physisorption data for gas/solid systems with special reference to the determination of surface area and porosity*. Pure & Appl. Chem., Vol. 57, No. 4, 603-619, 1985.
- 26 Dong, X., Liu, H., Hou, J., Wu, K., Chen, Z. *Phase Equilibria of Confined Fluids in Nanopores of Tight and Shale Rocks Considering the Effect of Capillary Pressure and Adsorption Film*. Ind. Eng. Chem. Res. 2016, 55, 3, 798–811.
- 27 Wang, L., Parsa, E., Gao, Y., Ok, J. T., Neeves, K., Yin, X., Ozkan, E. *Experimental Study and Modeling of the Effect of Nanoconfinement on Hydrocarbon Phase Behavior in Unconventional Reservoirs*. SPE-169581-MS.
- 28 Zhang, K., Jia, N., Liu, L. *Adsorption thicknesses of confined pure and mixing fluids in nanopores*. Langmuir 2018, 34, 12815-12826.
- 29 Qui, X., Tan, S. P., Dejam, M., Adidharma, H. *Simple and accurate isochoric differential scanning calorimetry measurements: phase transitions for pure fluids and mixtures in nanopores*. Phys. Chem. Chem. Phys., 2019, 21, 224-231.
- 30 Qui, X., Tan, S. P., Dejam, M., Adidharma, H. *Novel isochoric measurement of the onset of vapor–liquid phase transition using differential scanning calorimetry*. Phys. Chem. Chem. Phys., 2018, 20, 26241.